Hydromechanical modelling and numerical simulation of self-sealingphenomena in the Callovo-Oxfordian claystone

Joffrey Bluthé, B. Bary, Éric Lemarchand, Luc Dormieux

Hydromechanical modeling and numerical simulation of self-sealing phenomena in the Callovo-Oxfordian claystone

EGU - Session ERE5.5

Joffrey Bluthé[a,b], Benoît Bary[a], Eric Lemarchand[b], Luc Dormieux[b]

April, 13th 2018

[a]CEA, SECR, France
[b]Laboratoire Navier, ENPC, IFSTTAR, CNRS UMR 8205, Marne-La-Vallée, France

Contents

DE LA RECHERCHE À L'INDUSTRIE

Contents

Radioactive waste storage

Radioactive waste storage

- Roughly 72% of France's electricity production was nuclear in 2016

Radioactive waste storage

- Roughly 72% of France's electricity production was nuclear in 2016
- HLW represented 0.2% of the total volume of French radioactive waste but 94.98% of their total radioactivity in 2007

Radioactive waste storage

- Roughly 72% of France's electricity production was nuclear in 2016
- HLW represented 0.2% of the total volume of French radioactive waste but 94.98% of their total radioactivity in 2007
- Project Cigéo : HL/IL-LL waste repository

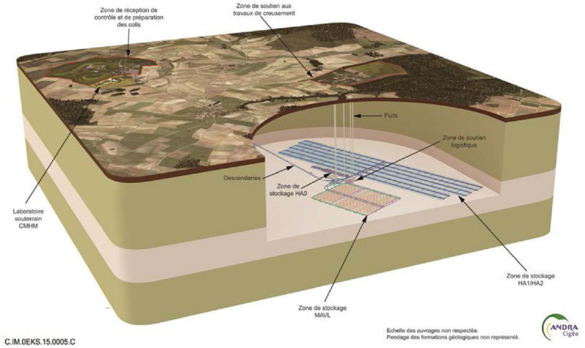

Damage and seals

DE LA RECHERCHE À L'INDUSTRIE

Damage and seals

- Excavation process leads to the creation of a high permeability damaged zone along the drifts

Damage and seals

- Excavation process leads to the creation of a high permeability damaged zone along the drifts

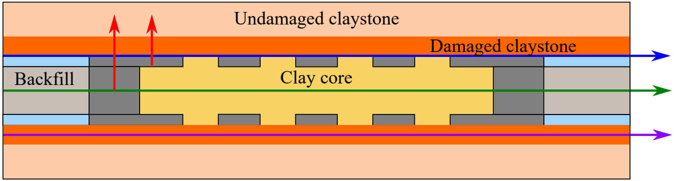

→ Transfer through interface between claystone, clay core and lining

→ Transfer through clay core and drifts

→ Transfer through damaged claystone

→ Transfer through Callovo-Oxfordian

Damage and seals

- Excavation process leads to the creation of a high permeability damaged zone along the drifts

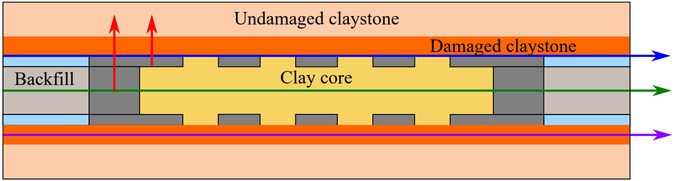

- Transfer through interface between claystone, clay core and lining (blue arrow)
- Transfer through clay core and drifts (green arrow)
- Transfer through damaged claystone (purple arrow)
- Transfer through Callovo-Oxfordian (red arrow)

- Goal for the overall hydraulic conductivity of the seals + galleries : $< 10^{-9}\ \mathrm{m \cdot s^{-1}}$ (Bauer et al. [2])

Self-sealing

Self-sealing

- **Self-sealing** = hydraulic conductivity drops dramatically when the claystone is hydrated

Self-sealing

- **Self-sealing** = hydraulic conductivity drops dramatically when the claystone is hydrated
- **Objective** : Predict the evolution of the damaged zone around a horizontal sealing during the resaturation phase

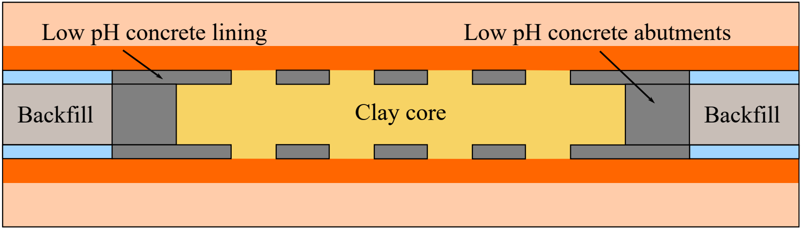

Self-sealing

- **Self-sealing** = hydraulic conductivity drops dramatically when the claystone is hydrated
- **Objective** : Predict the evolution of the damaged zone around a horizontal sealing during the resaturation phase

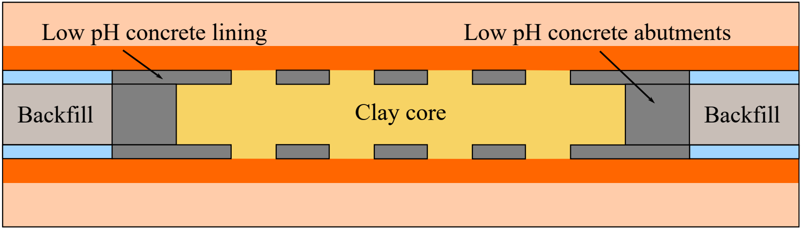

- **Hydromechanical coupling**

Self-sealing

- **Self-sealing** = hydraulic conductivity drops dramatically when the claystone is hydrated
- **Objective** : Predict the evolution of the damaged zone around a horizontal sealing during the resaturation phase

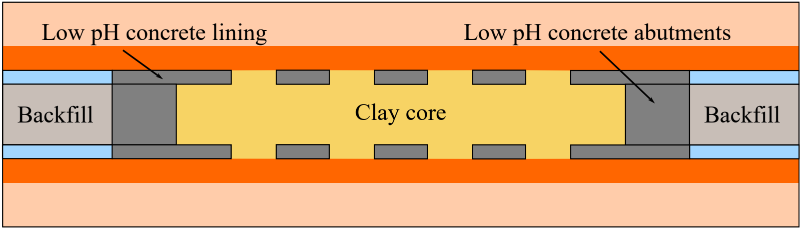

- **Hydromechanical coupling**
- Resaturation takes place over thousands of years ⇒ need to take into account the **viscoplastic** behavior of the claystone (not considered in the following, see perspectives)

Contents

Geometry

Geometry

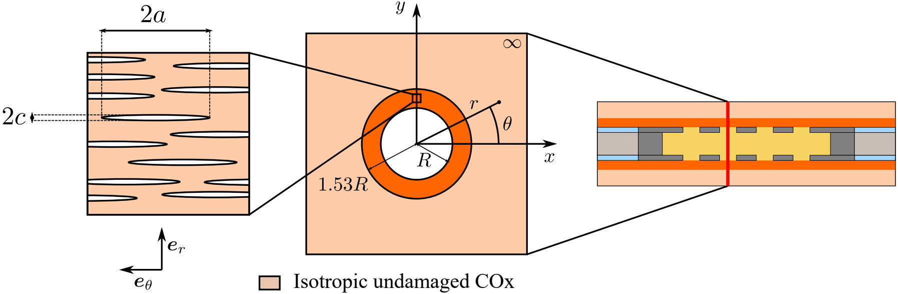

Isotropic undamaged COx

Transversely isotropic damaged COx

Geometry

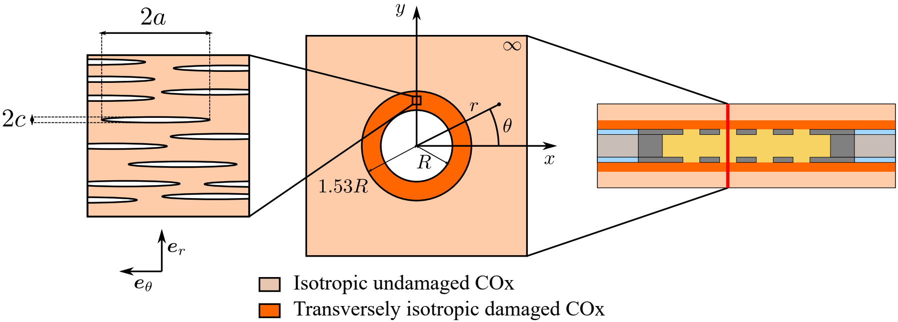

- Circular damaged zone with thickness $0.53R$ (ensures correct cross-sectional area)

Geometry

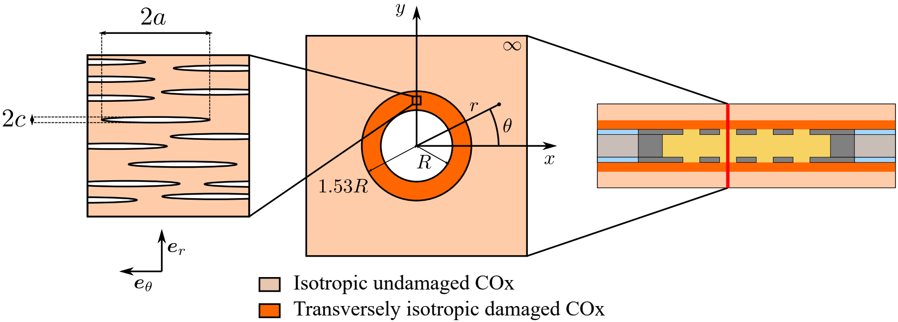

- Circular damaged zone with thickness $0.53R$ (ensures correct cross-sectional area)
- Mode I cracks parallel to the drift walls (normal = $\boldsymbol{e}_r$), mode II cracks disregarded

Material behavior and other hypotheses

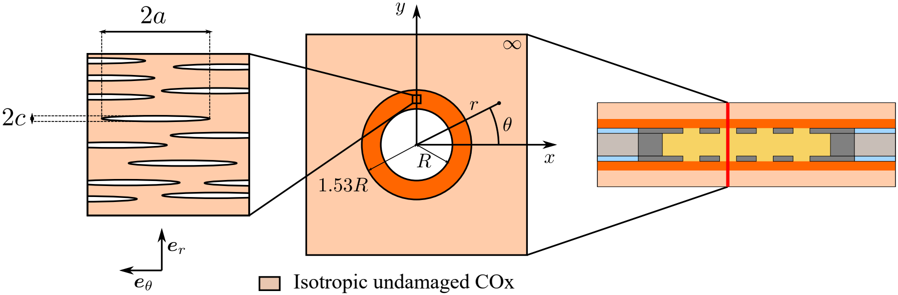

Isotropic undamaged COx

Transversely isotropic damaged COx

Material behavior and other hypotheses

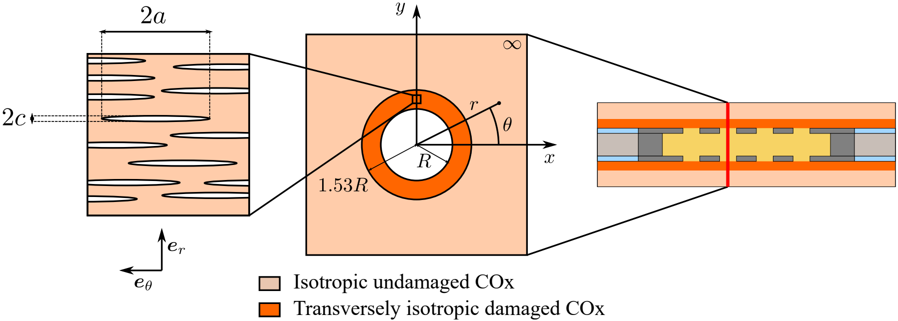

- Linear elastic isotropic behavior of the undamaged claystone

Material behavior and other hypotheses

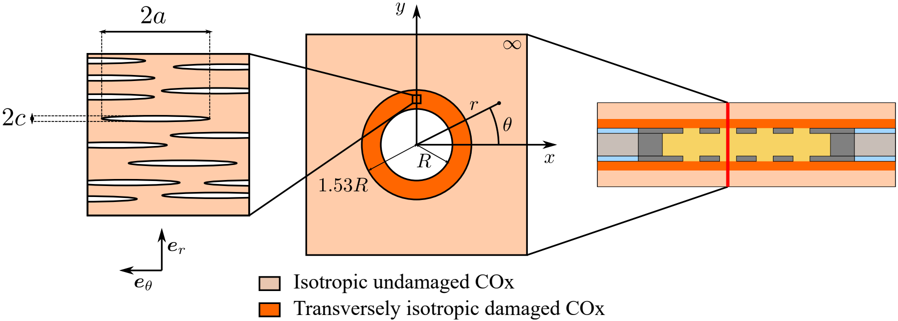

- Linear elastic isotropic behavior of the undamaged claystone
- No prestress

Material behavior and other hypotheses

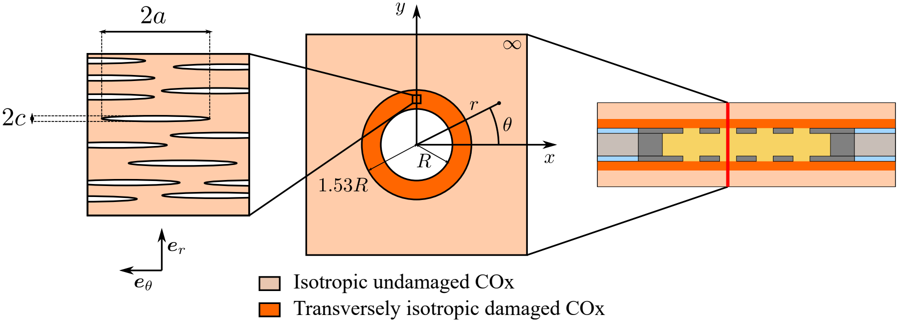

- Linear elastic isotropic behavior of the undamaged claystone
- No prestress
- Plane strain in the plane $\perp \boldsymbol{e}_z$

Material behavior and other hypotheses

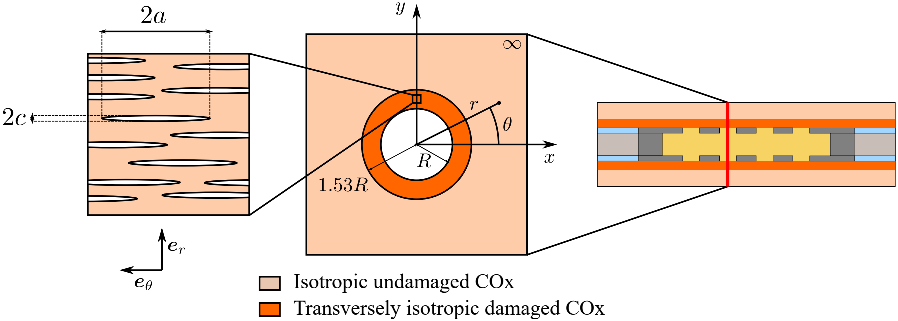

- Linear elastic isotropic behavior of the undamaged claystone
- No prestress
- Plane strain in the plane $\perp \boldsymbol{e}_z$
- Cracks remain open during the experiment (ensures linearity)

Loading and symmetry

Loading and symmetry

- Two kinds of loading in the CDZ experiment :

- Two kinds of loading in the CDZ experiment :
  - Problem (i) : $p = 4$ MPa pressure prescribed at $r = R$

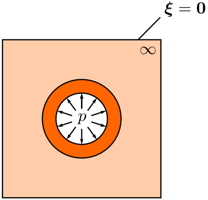

(a) Problem (i).

Loading and symmetry

- Two kinds of loading in the CDZ experiment :
  - Problem (i) : $p = 4$ MPa pressure prescribed at $r = R$
  - Problem (ii) : wetting and thus stress-free strain $\varepsilon^* = g(r)\mathbf{1}$ in the damaged zone, and $\boldsymbol{\sigma} \cdot \boldsymbol{n} = \mathbf{0}$ at $r = R$

    NB : Swelling leads to divergence of the drift walls and thus zero displacements at the boundary would lead to unrealistic surface tractions at $r = R$

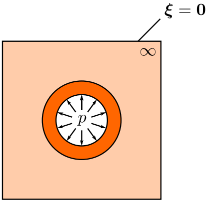

(a) Problem (i).

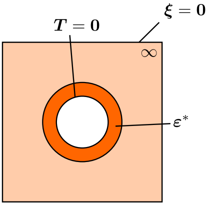

(b) Problem (ii).

Loading and symmetry

- Two kinds of loading in the CDZ experiment :
  - Problem (i) : $p = 4$ MPa pressure prescribed at $r = R$
  - Problem (ii) : wetting and thus stress-free strain $\boldsymbol{\varepsilon}^* = g(r)\mathbf{1}$ in the damaged zone, and $\boldsymbol{\sigma} \cdot \boldsymbol{n} = \mathbf{0}$ at $r = R$

    NB : Swelling leads to divergence of the drift walls and thus zero displacements at the boundary would lead to unrealistic surface tractions at $r = R$
- Geometry, material behavior, loading

  $\Rightarrow$ Rotational symmetry around $\boldsymbol{e}_z$

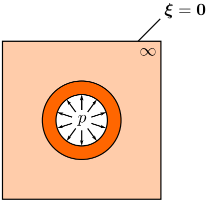

(a) Problem (i).

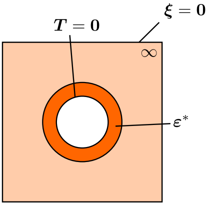

(b) Problem (ii).

Behavior of the damaged zone

Behavior of the damaged zone

- The homogenized behavior of the microcracked damaged zone is investigated in the rate form (ESHELBY based)

Behavior of the damaged zone

- The homogenized behavior of the microcracked damaged zone is investigated in the rate form (ESHELBY based)
- Linear elastic behavior of the intact claystone

$$\dot{\boldsymbol{\sigma}} = \mathbb{C}^{COx} : \left(\dot{\boldsymbol{\varepsilon}} - \dot{\boldsymbol{\varepsilon}}^*\right)$$

Behavior of the damaged zone

- The homogenized behavior of the microcracked damaged zone is investigated in the rate form (ESHELBY based)
- Linear elastic behavior of the intact claystone

$$\dot{\boldsymbol{\sigma}} = \mathbb{C}^{COx} : (\dot{\boldsymbol{\varepsilon}} - \dot{\boldsymbol{\varepsilon}}^*)$$

- Weak crack interaction : MORI-TANAKA scheme $\Rightarrow$ nonlinear elastic behavior of the microcracked damaged zone with the same stress-free strain

$$\dot{\boldsymbol{\Sigma}} = \mathbb{C}^{Dam}(\boldsymbol{\Sigma}) : \left(\dot{\boldsymbol{E}} - \dot{\boldsymbol{\varepsilon}}^*\right)$$

Behavior of the damaged zone

- The homogenized behavior of the microcracked damaged zone is investigated in the rate form (ESHELBY based)
- Linear elastic behavior of the intact claystone

$$\dot{\boldsymbol{\sigma}} = \mathbb{C}^{COx} : (\dot{\boldsymbol{\varepsilon}} - \dot{\boldsymbol{\varepsilon}}^*)$$

- Weak crack interaction : MORI-TANAKA scheme ⇒ nonlinear elastic behavior of the microcracked damaged zone with the same stress-free strain

$$\dot{\boldsymbol{\Sigma}} = \mathbb{C}^{Dam}(\boldsymbol{\Sigma}) : \left(\dot{\boldsymbol{E}} - \dot{\boldsymbol{\varepsilon}}^*\right)$$

- The crack opening variation is derived (Deudé [5]) :

$$\dot{c} = c\left(\dot{\overline{\boldsymbol{\varepsilon}}}^c : \boldsymbol{n} \otimes \boldsymbol{n}\right) = aX\left(\dot{\overline{\boldsymbol{\varepsilon}}}^c : \boldsymbol{n} \otimes \boldsymbol{n}\right)$$

The flat spheroid limit

The flat spheroid limit

- Cracks $\rightarrow X = \frac{c}{a} \ll 1$ (same X for all cracks)

The flat spheroid limit

- Cracks $\rightarrow X = \frac{c}{a} \ll 1$ (same X for all cracks)
- This leads to

$$\mathbb{C}^{Dam} = \mathbb{C}^{COx} : \left(\mathbb{I} + \frac{4\pi}{3} d\mathbb{T} \right)^{-1} \quad ; \quad \mathbb{T}(\nu^{COx})$$

The flat spheroid limit

- Cracks $\rightarrow X = \frac{c}{a} \ll 1$ (same X for all cracks)
- This leads to

$$\mathbb{C}^{Dam} = \mathbb{C}^{COx} : \left(\mathbb{I} + \frac{4\pi}{3} d\mathbb{T}\right)^{-1} \quad ; \quad \mathbb{T}(\nu^{COx})$$

- $d = \mathcal{N} a^3$ is the crack density parameter (Budiansky and O'connell [3])

The flat spheroid limit

- Cracks $\to X = \frac{c}{a} \ll 1$ (same X for all cracks)
- This leads to

$$\mathbb{C}^{Dam} = \mathbb{C}^{COx} : \left(\mathbb{I} + \frac{4\pi}{3} d\mathbb{T}\right)^{-1} \quad ; \quad \mathbb{T}(\nu^{COx})$$

- $d = \mathcal{N} a^3$ is the crack density parameter (Budiansky and O'connell [3])
- In that limit the problem is linear (as long as the cracks remain open) because $\mathbb{C}^{Dam}$ is independent of $c \Rightarrow$ integration with respect to time is possible

The flat spheroid limit

- Cracks $\rightarrow X = \frac{c}{a} \ll 1$ (same X for all cracks)
- This leads to

$$\mathbb{C}^{Dam} = \mathbb{C}^{COx} : \left(\mathbb{I} + \frac{4\pi}{3} d\mathbb{T}\right)^{-1} \quad ; \quad \mathbb{T}(\nu^{COx})$$

- $d = \mathcal{N} a^3$ is the crack density parameter (Budiansky and O'connell [3])
- In that limit the problem is linear (as long as the cracks remain open) because $\mathbb{C}^{Dam}$ is independent of $c \Rightarrow$ integration with respect to time is possible
- Also

$$\begin{aligned} \dot{c} &= \left[\mathbb{T} : \left(\mathbb{I} + \frac{4\pi}{3} d\mathbb{T}\right)^{-1} : \left(\dot{\boldsymbol{E}} - \dot{\boldsymbol{\varepsilon}}^*\right)\right] : (a\boldsymbol{n} \otimes \boldsymbol{n}) \\ &= \left[\mathbb{T} : \mathbb{C}^{COx-1} : \dot{\boldsymbol{\Sigma}}\right] : (a\boldsymbol{n} \otimes \boldsymbol{n}) \end{aligned}$$

Boundary value problem

Boundary value problem

- Integrated equations (no propagation of cracks) :

$$\begin{cases} \boldsymbol{\Sigma} = \mathbb{C}^{Dam} : (\boldsymbol{E} - \boldsymbol{\varepsilon}^*) \\ \Delta X = \frac{\Delta c}{a} = \left[\mathbb{T} : \mathbb{C}^{COx-1} : \boldsymbol{\Sigma} \right] : (\boldsymbol{n} \otimes \boldsymbol{n}) \end{cases}$$

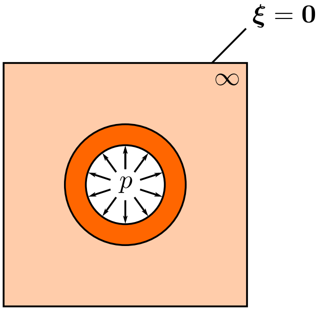

(a) Problem (i) : prescribed pressure.

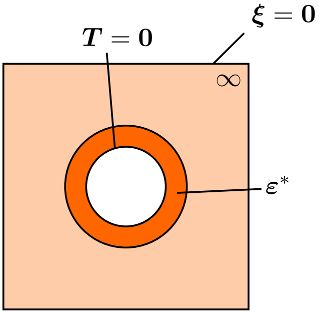

(b) Problem (ii) : prescribed stress-free strain.

Analytical solution

Analytical solution

- Rotational symmetry $\Rightarrow$ total displacement looked for in the form $\boldsymbol{\xi} = f(r)\boldsymbol{e}_r$

Analytical solution

- Rotational symmetry $\Rightarrow$ total displacement looked for in the form $\boldsymbol{\xi} = f(r)\boldsymbol{e}_r$
- Equation of equilibrium yields a second order ordinary differential equation

Analytical solution

- Rotational symmetry $\Rightarrow$ total displacement looked for in the form $\boldsymbol{\xi} = f(r)\boldsymbol{e}_r$
- Equation of equilibrium yields a second order ordinary differential equation
- Exact analytical solution if $g(r)$ is a polynomial function of r

Analytical solution

- Rotational symmetry $\Rightarrow$ total displacement looked for in the form $\boldsymbol{\xi} = f(r)\boldsymbol{e}_r$
- Equation of equilibrium yields a second order ordinary differential equation
- Exact analytical solution if $g(r)$ is a polynomial function of r
- If g is only assumed to be continuous, it can be approximated by a polynomial function $\Rightarrow$ yields an approximate solution

Parameters

Parameter	Value	Reference
E^{COx} (MPa)	5000	Pham [7]*
ν^{COx} (-)	0.2	Pham [7]*
d (-)	10^{-3}	arbitrary
ε^* (-)	10^{-2}	Zhang et al. [8]**
$p^{swelling}$ (MPa)	4	Andra [1]

*These are averaged values estimated using the measurements before desaturation and after resaturation

**This is the average prescribed strain over the damaged zone. Much higher strains are observed under free swelling conditions and much lower under high triaxial confining stresses so a conservative value of 1% was chosen

Results

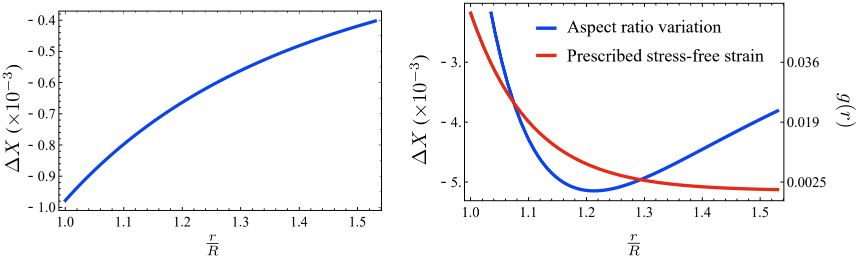

(a) Problem (i).

(b) Problem (ii).

FIGURE – ΔX as a function of $\frac{r}{R}$ for problems (i) and (ii).

Results

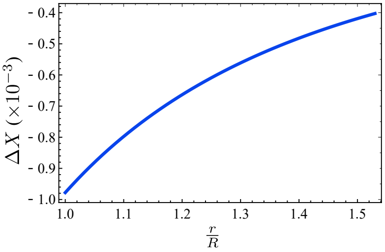

(a) Problem (i).

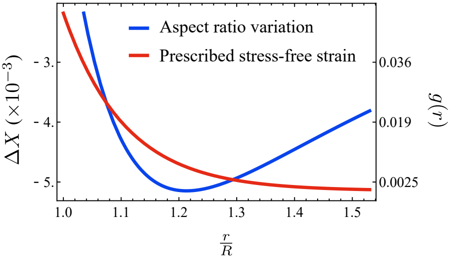

(b) Problem (ii).

FIGURE – ΔX as a function of $\frac{r}{R}$ for problems (i) and (ii).

$|\Delta X|$ max is roughly five times greater for problem (ii) than for problem (i)

Influence of $g(r)$

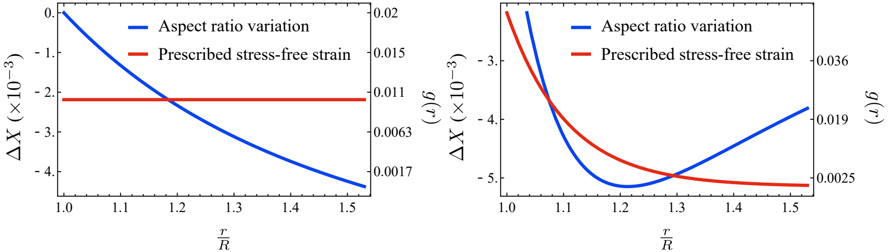

(a) Homogeneous stress-free strain.

(b) Exponentially decaying stress-free strain.

FIGURE – ΔX as a function of $\frac{r}{R}$ for two different functions $g(r)$ with the same average value.

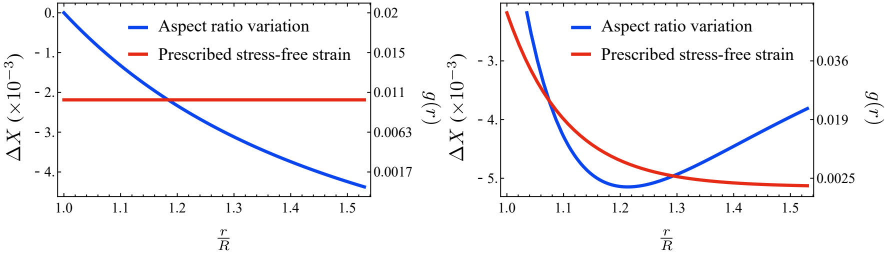

(a) Homogeneous stress-free strain. (b) Exponentially decaying stress-free strain.

FIGURE – ΔX as a function of $\frac{r}{R}$ for two different functions $g(r)$ with the same average value.

Different monotony but same order of magnitude for $|\Delta X|$ max

A word on a and d

A word on a and d

- Note that $|\Delta X|$ max does not depend much on d for problem (ii) ($5.023 \cdot 10^{-3}$ for $d = 10^{-1}$ and $5.148 \cdot 10^{-3}$ for $d = 10^{-6}$) and even less for problem (i) ($9.77848 \cdot 10^{-4}$ in both cases) so a median value of 10^{-3} was chosen arbitrarily

A word on a and d

- Note that $|\Delta X|$ max does not depend much on d for problem (ii) ($5.023 \cdot 10^{-3}$ for $d = 10^{-1}$ and $5.148 \cdot 10^{-3}$ for $d = 10^{-6}$) and even less for problem (i) ($9.77848 \cdot 10^{-4}$ in both cases) so a median value of 10^{-3} was chosen arbitrarily
- Taking the value $a = 250$ mm (Hawkins et al. [6]) for the lateral extent of the cracks yields crack opening variations of -0.5 mm and -2.6 mm for problems (i) and (ii) respectively

A word on a and d

- Note that $|\Delta X|$ max does not depend much on d for problem (ii) ($5.023 \cdot 10^{-3}$ for $d = 10^{-1}$ and $5.148 \cdot 10^{-3}$ for $d = 10^{-6}$) and even less for problem (i) ($9.77848 \cdot 10^{-4}$ in both cases) so a median value of 10^{-3} was chosen arbitrarily
- Taking the value $a = 250$ mm (Hawkins et al. [6]) for the lateral extent of the cracks yields crack opening variations of -0.5 mm and -2.6 mm for problems (i) and (ii) respectively
- This is consistent with *in situ* observations of initial crack openings on the order of the millimeter

Contents

Conclusions

Conclusions

- Simple model but yields interesting insights into the phenomenon of self-sealing at the scale of the drift

Conclusions

- Simple model but yields interesting insights into the phenomenon of self-sealing at the scale of the drift
- The crack closure was found to be a non-monotonous function of depth for an exponentially decaying stress-free strain

Conclusions

- Simple model but yields interesting insights into the phenomenon of self-sealing at the scale of the drift
- The crack closure was found to be a non-monotonous function of depth for an exponentially decaying stress-free strain
- A mean 1% stress-free strain was found to lead to better self-sealing than the 4 MPa swelling pressure developed by the swelling clay core

Conclusions

- Simple model but yields interesting insights into the phenomenon of self-sealing at the scale of the drift
- The crack closure was found to be a non-monotonous function of depth for an exponentially decaying stress-free strain
- A mean 1% stress-free strain was found to lead to better self-sealing than the 4 MPa swelling pressure developed by the swelling clay core
- Results consistent with *in situ* observation that water injection is more efficient than pure mechanical closure

Perspectives

Perspectives

- The damaged zone was represented by an effective microcracked medium with weak interaction $\rightarrow$ strong interaction could be dealt with by using a self-consistent scheme, but more importantly the cracks should be introduced explicitly at the scale of the drift

DE LA RECHERCHE À L'INDUSTRIE

Perspectives

- The damaged zone was represented by an effective microcracked medium with weak interaction $\rightarrow$ strong interaction could be dealt with by using a self-consistent scheme, but more importantly the cracks should be introduced explicitly at the scale of the drift
- The actual problem is nonlinear due to the closure of different families of cracks

Perspectives

- The damaged zone was represented by an effective microcracked medium with weak interaction $\rightarrow$ strong interaction could be dealt with by using a self-consistent scheme, but more importantly the cracks should be introduced explicitly at the scale of the drift
- The actual problem is nonlinear due to the closure of different families of cracks
- The stress-free strain was prescribed, when it is in fact the result of a coupled hydromechanical response (the amount of water a sample is able to take in depends on the confining stress which in turn depends on the swelling)

Perspectives

- The damaged zone was represented by an effective microcracked medium with weak interaction $\rightarrow$ strong interaction could be dealt with by using a self-consistent scheme, but more importantly the cracks should be introduced explicitly at the scale of the drift
- The actual problem is nonlinear due to the closure of different families of cracks
- The stress-free strain was prescribed, when it is in fact the result of a coupled hydromechanical response (the amount of water a sample is able to take in depends on the confining stress which in turn depends on the swelling)
- Time effects have to be included at the scale of the clay particles ($\simeq 10 - 50$ nm), resulting behavior will be used at the scale of the drift

Thank you for your attention.

References I

[1] Andra. Dossier d'options de sûreté - Partie après fermeture (DOS-AF), 2016. 50

[2] C Bauer, G Pépin, and P Lebon. Edz in the performance assessment of the meuse/haute-marne site : conceptual model used and questions addressed to the research. In *Proceedings of the European Commission Cluster conference on Impact of the EDZ on the performance of radioactive waste geological repositories, Luxembourg November*, volume 40, 2003. 8, 9, 10, 11

[3] Bernard Budiansky and Richard J O'connell. Elastic moduli of a cracked solid. *International journal of Solids and structures*, 12(2) :81–97, 1976. 37, 38, 39, 40, 41, 42

[4] Rémi de La Vaissière, Gilles Armand, and Jean Talandier. Gas and water flow in an excavation-induced fracture network around an underground drift : a case study for a radioactive waste repository in clay rock. *Journal of Hydrology*, 521 :141–156, 2015.

[5] Vincent Deudé. *Non linéarités géométriques et physiques dans les milieux poreux : apport des méthodes de changement d'échelle*. PhD thesis, Ecole des Ponts ParisTech, 2002. 32, 33, 34, 35, 36

References II

[6] IR Hawkins, BT Swift, AR Hoch, and J Wendling. Comparing flows to a tunnel for single porosity, double porosity and discrete fracture representations of the edz. *Physics and Chemistry of the Earth, Parts A/B/C*, 36(17) :1990–2002, 2011. 55, 56, 57, 58

[7] Quoc Thai Pham. *Effets de la désaturation et de la resaturation sur l'argilite dans les ouvrages souterrains.* PhD thesis, Ecole Polytechnique X, 2006. 50

[8] CL Zhang, K Wieczorek, and ML Xie. Swelling experiments on mudstones. *Journal of Rock Mechanics and Geotechnical Engineering*, 2(1) :44–51, 2010. 50